Supporting information for: Influence of cobalt substitution on the magnetic properties of Fe_5PB_2

Johan Cedervall,[*,†] Elise Nonnet,[†] Daniel Hedlund,[‡] Lennart Häggström,[¶] Tore Ericsson,[¶] Mirosław Werwiński,[§] Alexander Edström,[¶,‖] Ján Rusz,[¶] Peter Svedlindh,[‡] Klas Gunnarsson,[‡] and Martin Sahlberg[†]

†*Department of Chemistry - Ångström Laboratory, Uppsala University, Box 538, 751 21 Uppsala, Sweden.*

‡*Department of Engineering Sciences, Uppsala University, Box 534, 751 21 Uppsala, Sweden.*

¶*Department of Physics and Astronomy, Uppsala University, Box 516, 751 20 Uppsala, Sweden*

§*Institute of Molecular Physics Polish Academy of Sciences, M. Smoluchowskiego 17, 60-179 Poznań, Poland*

‖*Department of Materials Theory, ETH Zürich, Wolfgang-Pauli-Str. 27, 8093 Zürich, Switzerland*

E-mail: johan.cedervall@kemi.uu.se

Table S1: R_{Bragg} and χ^2 values for all refined XRD powder patterns. The R_{Bragg} values are given for the main phase ($(Fe_{1-x}Co_x)_5PB_2$).

x	R_{Bragg}	χ^2
0	6.11	1.39
0.1	3.40	1.43
0.2	6.77	1.89
0.3	5.24	1.55
0.4	5.15	1.41
0.5	6.22	1.50
0.6	7.92	1.51
0.7	6.22	1.28

Table S2: Refined unit cell parameters for the $(Fe_{1-x}Co_x)_5PB_2$ main phase for $x \leq 0.7$ including unit cell volume and c/a-ratio.

x	a (Å)	c (Å)	V (Å^3)	c/a
0	5.4923(1)	10.3654(4)	312.67(2)	1.8873(4)
0.1	5.4792(2)	10.3711(6)	311.36(3)	1.8928(6)
0.2	5.4601(3)	10.3702(8)	309.16(5)	1.8993(9)
0.3	5.4404(4)	10.3682(10)	306.88(5)	1.9058(11)
0.4	5.4322(2)	10.3674(4)	305.93(2)	1.9085(4)
0.5	5.4209(1)	10.3594(3)	304.42(2)	1.9110(3)
0.6	5.4075(2)	10.3504(7)	302.66(3)	1.9141(7)
0.7	5.4020(2)	10.3324(6)	301.48(3)	1.9127(6)

Table S3: Fitting for spectra of Fe_5PB_2 ($x = 0$) and $Fe_{4.5}Co_{0.5}PB_2$ ($x = 0.1$) at 295 K. B is the magnetic hyperfine field in T, CS is the central shift in mm/s, dQ is the electric quadrupole shift in mm/s, I is the spectral intensity in % and W is the Lorentzian line width (full width at half maximum) in mm/s. Errors in CS, dQ and W are ± 0.01 mm/s and in B is ± 0.1 T.

*dQ is the first order electric quadrupole perturbation term for dominating magnetic interaction, $dQ = \frac{eQV_{zz}}{2}\left(\frac{3\cos^2\theta - 1 + \eta\sin^2\theta\cos 2\phi}{2}\right)$. Here Q is the nuclear electric quadrupole moment of the excited state of ^{57}Fe, V_{zz} the principal component of the electric field gradient (EFG) tensor, θ and ϕ the polar and azimuthal angles of the principal axis z of the EFG versus the magnetic hyperfine field and η the asymmetry parameter of the EFG tensor.

	Fe(1)a				Fe(1)b				Fe(2)				
x	B	CS	dQ	I	B	CS	dQ	I	B	CS	dQ	I	W
0	14.8	0.35	-0.03	71(2)	18.1	0.34	-0.02	8(2)	20.1	0.12	0.82	21(2)	0.22
0.1	13.9	0.35	-0.02	82(2)	17.4	0.35	0.08	3(2)	19.3	0.11	0.82	12(2)	0.24

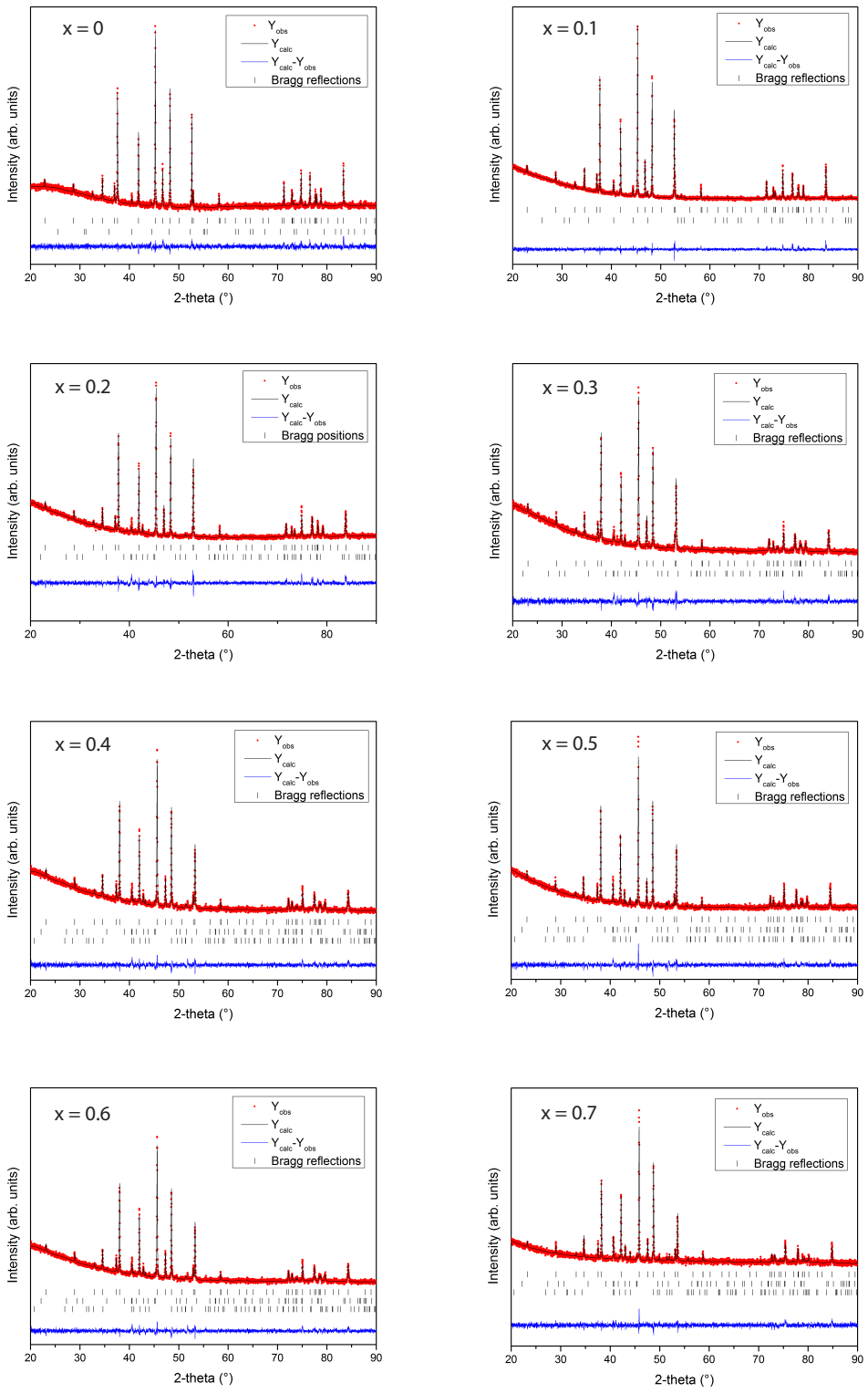

Figure S1: Refined XRD powder patterns for all compositions in $(Fe_{1-x}Co_x)_5PB_2$ for $x \leq 0.7$. The secondary phases are Fe_2P, $Fe_3P_{0.64}B_{0.36}$ and Co_2P.

Table S4: Results from the fitting of the paramagnetic spectra. CS, QS and W are given in mm/s, the temperature T in K and the spectral intensity I in %. QS is the magnitude of the electric quadrupole splitting, $QS = \left|\frac{eQV_{zz}}{2} \cdot \sqrt{1+\frac{\eta^3}{3}}\right|$. Errors in CS, QS and W are $\pm$ 0.01 mm/s.

		Fe(1)			Fe(2)			Fe impurity			
x	T	CS	QS	I	CS	QS	I	CS	QS	I	W
0**	900	-0.10	0.35	79(2)	-0.33	0.57	21(2)			-	0.29
0.1	580	0.13	0.37	82(2)	-0.16	0.67	18(2)			-	0.25
0.2	524	0.16	0.36	69(2)	-0.11	0.74	22(2)	0.37	0.79	9(2)	0.27
0.3	437	0.22	0.36	72(2)	-0.05	0.78	19(2)	0.47	0.90	10(2)	0.28
0.4	402	0.23	0.34	87(2)	0.06	0.91	13(2)			-	0.27
0.5	295	0.33	0.34	87(2)	0.10	0.79	13(2)			-	0.27
0.6	295	0.33	0.30	86(2)	0.14	0.86	6(2)	0.52	0.90	8(2)	0.23
0.7	295	0.33	0.30	85(2)	0.15	0.91	3(2)	0.52	0.90	12(2)	0.24

** values taken from ref. (11).

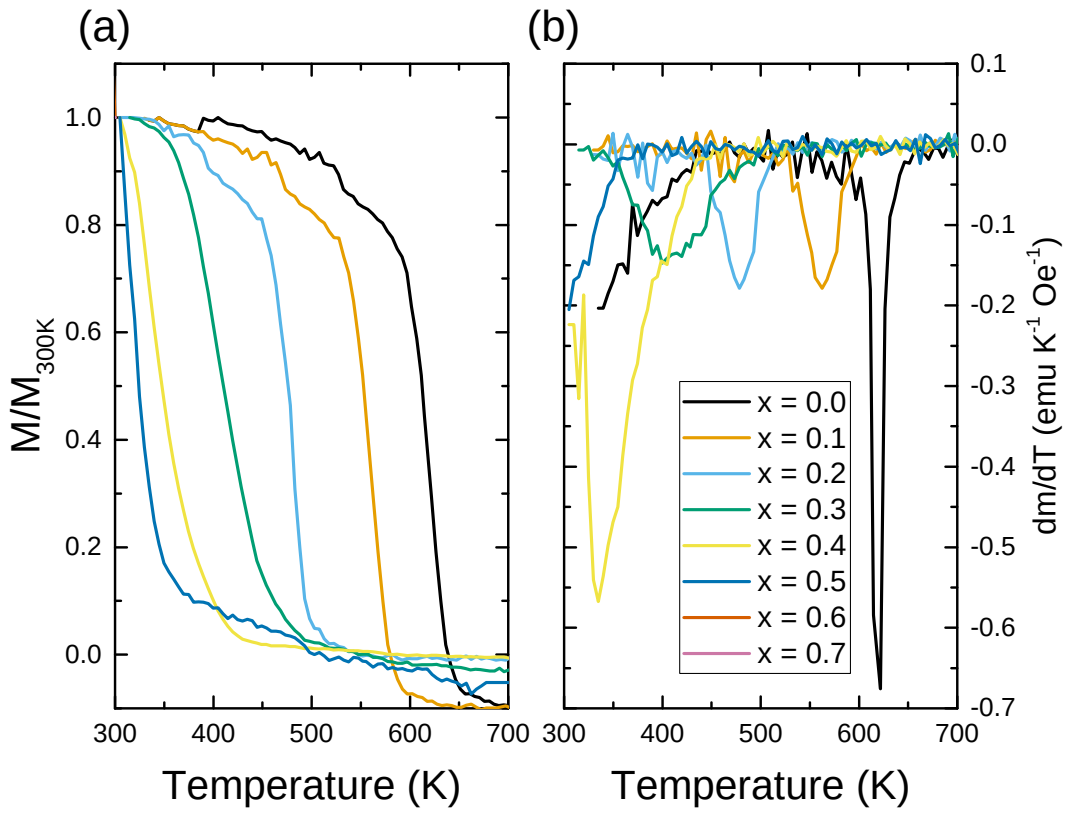

Figure S2: Field cooled measurements between 300 and 700 K under an applied field of μ_0H = 0.01 T. (a) Magnetization divided by the magnetization at 300 K. (b) Differential magnetization.

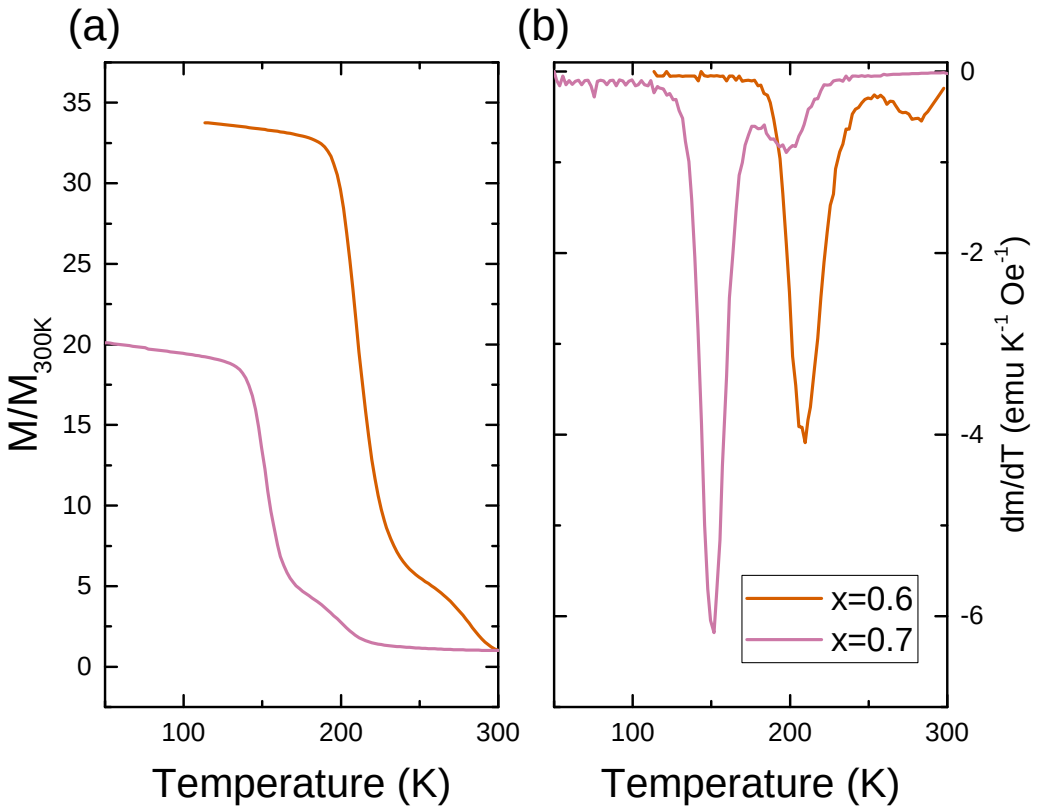

Figure S3: Field cooled measurements between 3 and 300 K under an applied field of μ_0H = 0.01 T. (a) Magnetization divided by the magnetization at 300 K. (b) Differential magnetization.

Table S5: Saturation magnetization (M_{sat}) at 3 and 300 K and Curie temperature (T_C) by the inflection point of field cooled measurements in a field of μ_0H = 0.1 T and 0.01 T.

x	M_{sat} 3 K (MA/M)	M_{sat} 300 K (MA/M)	T_C 0.01 T (K)	T_C 0.1 T (K)
0.0	0.98305	0.83218	622	638
0.1	0.89334	0.73137	563	562
0.2	0.78747	0.63640	481	476
0.3	0.71290	0.51283	400	392
0.4	0.60505	0.36409	335	326
0.5	0.53887	0.20303	278	274
0.6	0.45072	NA (0.05511)	209	209
0.7	0.17924	NA (0.04335)	152	152

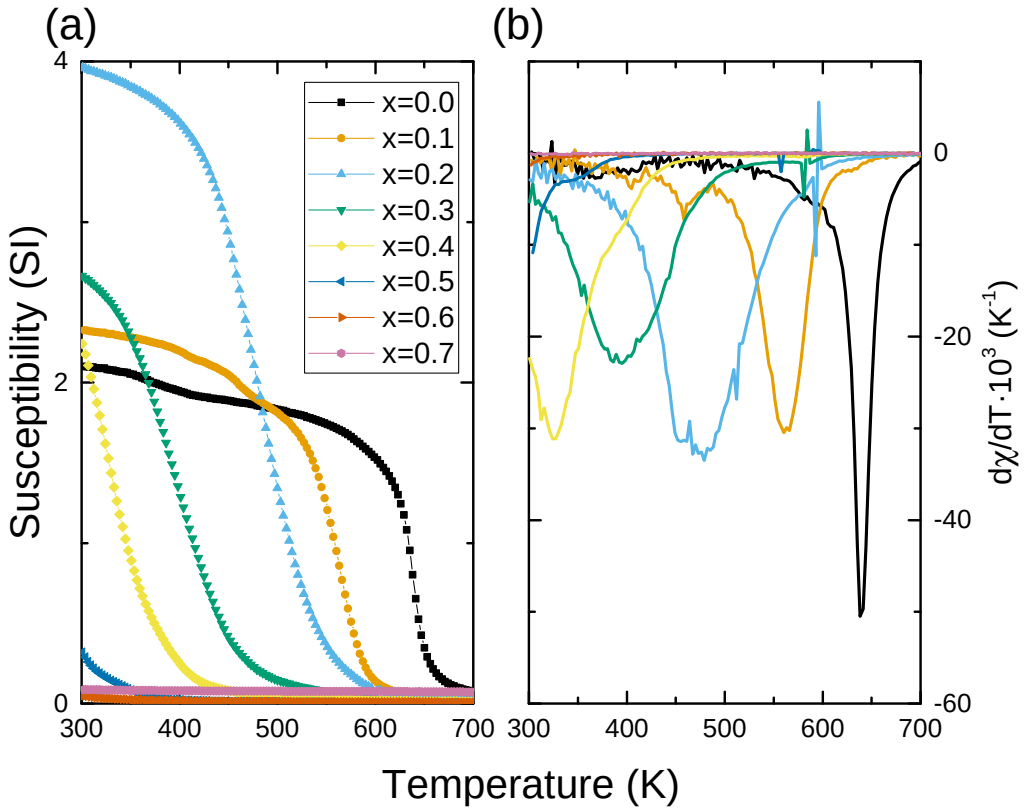

Figure S4: Field cooled measurements between 300 and 700 K under an applied field of μ_0H = 0.1 T. (a) Magnetic susceptibility in SI units. (b) Differential susceptibility.

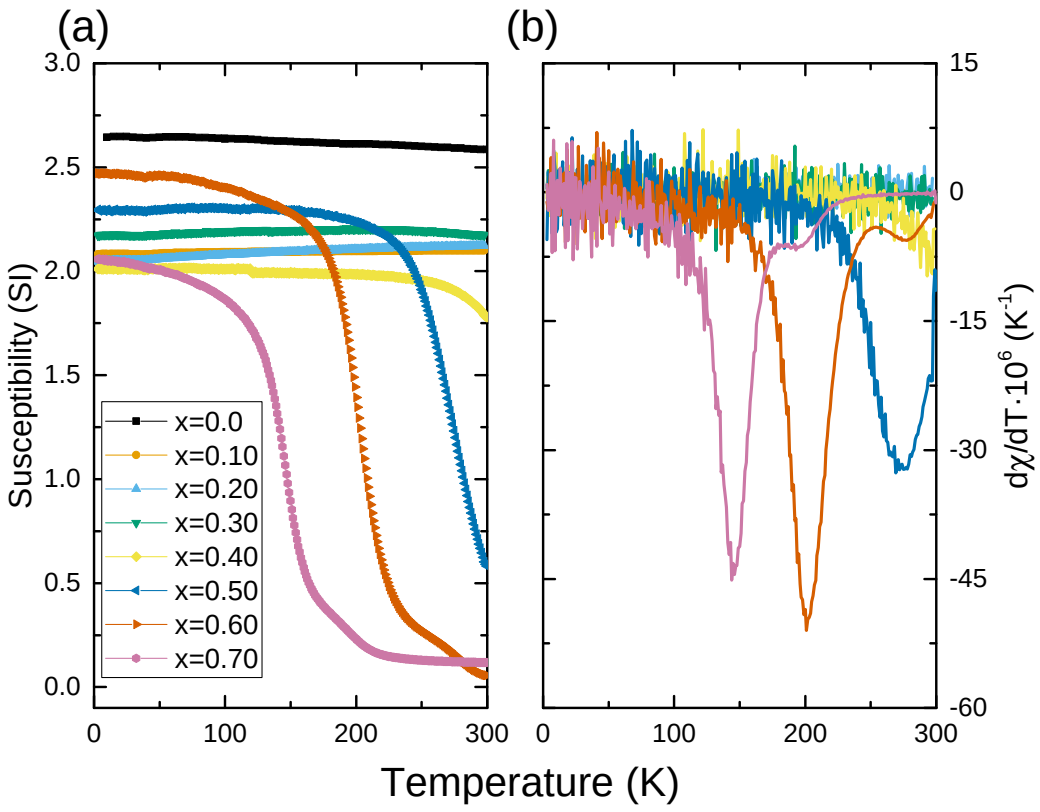

Figure S5: Field cooled measurements between 3 and 300 K under an applied field of μ_0H = 0.1 T. (a) Magnetic susceptibility in SI units. (b) Differential susceptibility.

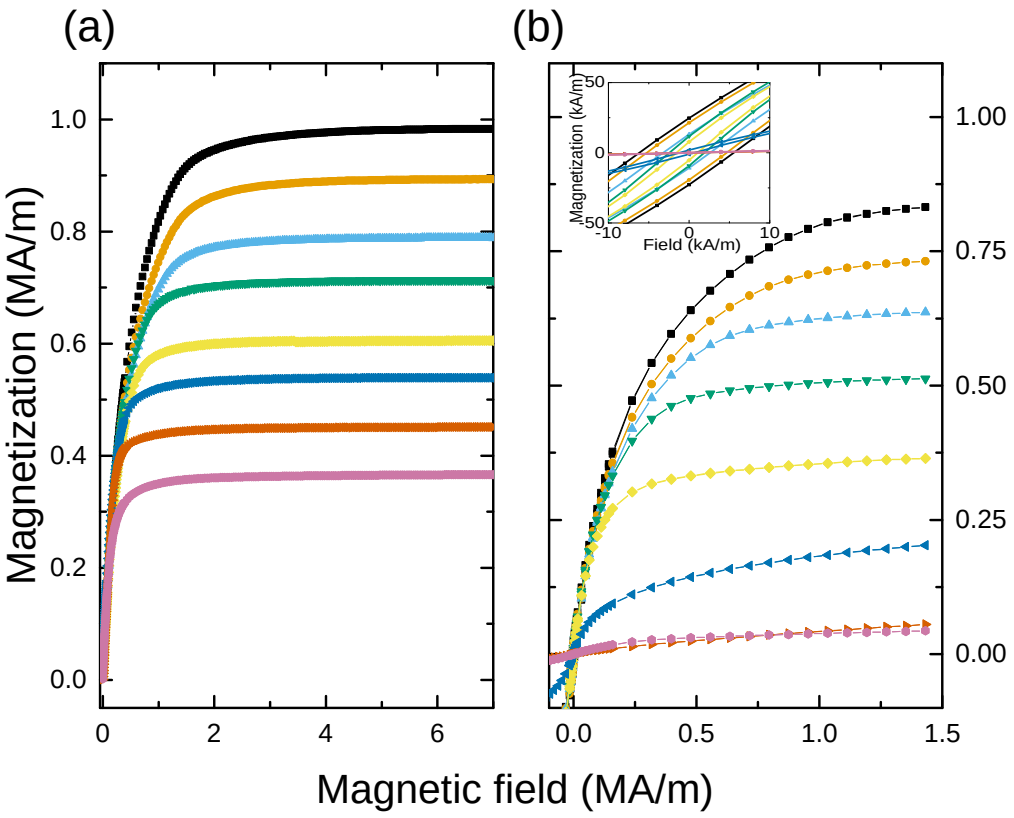

Figure S6: M–H curves for $x = 0.0$ (top) to $x = 0.70$ (bottom). (a) At T = 3 K and (b) At room temperature. The insert shows the neglible remanence and coercivity of the samples.